Study of design parameters of flapping-wings

Q. Wang*, J.F.L. Goosen, and F. van Keulen
Structural Optimization & Mechanics Group
Faculty of Mechanical, Maritime and Materials Engineering
Delft University of Technology, Delft, The Netherlands

ABSTRACT

As one of the most important components of a flapping-wing micro air vehicle (FWMAV), the design of an energy-efficient flapping-wing has been a research interest recently. Research on insect flight from different perspectives has been carried out, mainly with regard to wing morphology, flapping kinematics, and unsteady aerodynamics. However, the link between the wing morphology and kinematics with passive pitching has been neglected in flapping-wing design. To address this, a model based on a quasi-steady aerodynamic model and the passive pitching motion was made. To simplify the model and make optimization more feasible, the wing is modeled as a stiff plate with uniform mass distribution and a torsional spring at the wing root. An optimization is conducted with the objective of minimizing power consumption for hovering flight using the six most influential wing morphological and kinematic parameters as design variables. The sensitivity of lift generation and power consumption to all the parameters is analyzed. Compared to traditional artificial wings with straight leading edges as pitching axis, wings with a part of wing area in front of the pitching axis and smaller aspect ratio are able to perform more energy-efficient hovering flights. Preliminary design suggestions regarding the selection of wing shape and kinematics for FWMAVs are given.

1 INTRODUCTION

Inspired by gliding birds, engineers designed airplanes equipped with fixed wings to fly when moving at a high speed through the air. This design concept has proved successful in long-distance transport, but has bad performance in the low-speed range and is useless for hovering. The helicopter designs solve this with rotary wings providing the possibility to hover and move slowly. However, when we reduce the size of helicopters to execute tasks in limited space, the noise from fast rotating blades becomes a big issue and the collision with other objects is often fatal. Given aforementioned reasons, designers switched to mimic the flapping flight of birds and insects since they are the specialists in nature on slow and agile flight especially with small body sizes. Several kinds of flapping-wing micro air vehicles (FWMAVs) [1, 2, 3] were designed by mimicking insect flight, which requires less control of the wing itself compared to bird flight.

As a dominant part for the generation of lift and thrust, study on the flapping-wings of insects has been conducted from perspectives of wing morphology, kinematics, unsteady aerodynamics, etc. Biologists have observed insect flight for centuries and studied the wing morphology a lot in the early days. Ellington [4] studied the relation between the radii of wing area for a variety of insects, birds and bats, and found that wings of flying animals adhere to "laws of shape", implying the possibility for analytical representation of the spanwise wing area distribution. Wootton [5] elaborately studied and summarized the functionality of insect wing morphology. The combination of wing venation and membrane determines the spanwise stiffness to avoid excessive wing bending but allows a certain spanwise flexibility for wing pitching and torsion. This morphological characteristic facilitates the generation of expected kinematics for energy-efficient flight with the help of wing inertial and aerodynamic loads. Several studies [6, 7, 8] have investigated why insects adopt certain kinematics from the aerodynamic performance and energy efficiency perspectives. Numerous optimization for the flapping-wing kinematics were also used to strengthen the understanding of insect flights [9, 10] and assist the design of FWMAVs [11, 12].

Although research has focused both on wing morphology and flapping kinematics, little work has been carried out to systematically study the morphological and kinematic parameters simultaneously. Insects with different wing morphology generally flap in different ways, which reflects the mutual relationship between wing morphology and kinematics. This can be partly attributed to the fact that most insects make use of passive pitching [13, 14], and the passive pitching is determined by both the wing morphology and flapping motion. Additionally, kinematics with passive pitching are also preferable for FWMAVs since this simplifies the drive mechanism and, thus, reduces the total mass. Thus, it is necessary to do a combined analysis of both wing morphological and flapping kinematic parameters while the pitching motion is passive. As the kinematics are strongly dependent on the flight mode, a specific flight mode must be chosen for the analysis. This paper concentrates on hovering flight for two

*Q.Wang-3@tudelft.nl

reasons. First, insects and FWMAVs exhibit a variety of forward flights with different forward speeds, flight trajectories and objectives (e.g., for maximum flying time or distance). This variation makes the forward flight hard to specify for quantitative analysis. In contrast, most hovering flights share the same objective: minimal power consumption (or maximal hovering time). Second, hovering flight is a requisite capability for most insects and FWMAVs, and it requires more energy than forward flight in intermediate speed [8], which implies the importance of studying hovering flight to reduce the overall energy expenditure.

In this paper, wing morphological and kinematic parameters are first described in detail. Then, with preliminary analysis of these parameters, the most influential ones are selected as design variables for optimization. Finally, based on the optimal combination of wing shape and kinematics, single parameter sensitivities of lift and power consumption are calculated and analyzed.

2 Design Parameters

Insect wings are thin cuticular structures that consist of membranous regions of epidermal bilayers reinforced by veins [15]. The veins are used to maintain the wing shape and facilitate the aerodynamic loads generation. To this end, they increase the spanwise stiffness to reduce wing bending but allow chordwise flexibility that permits the twisting necessary to achieve the required angles of attack.

Instead of pitching the wing with distributed flexibility, we mimic the passive pitching motion by connecting a rigid wing to a torsional spring, as shown in Figure 1. Ignoring the deformation of the wing itself and, thus, the influence of wing bending, torsion and chamber, the morphological parameters are reduced to pure wing shape parameters.

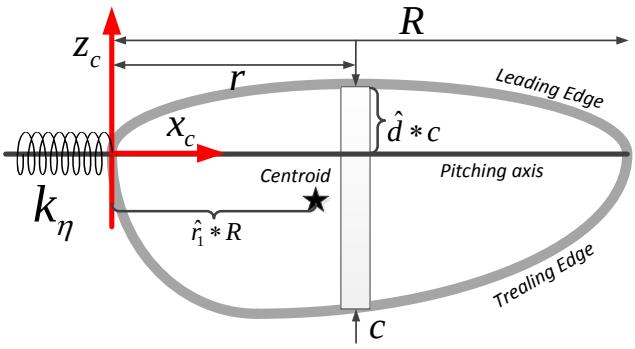

Figure 1: Illustration of the wing model with a detailed description of shape parameters.

2.1 Wing morphological parameters

To quantitatively describe a wing shape, the line from the wing root to tip is defined as a reference line. This line is also assumed to be the pitching axis in the kinematics description. Next, the leading edge (LE) and trailing edge (TE) can be identified clearly, as shown in Figure 1.

The wing area (S) enclosed by the LE and TE has the most significant influence on the lift and trust generation, and is conventionally quantified with the wing span (R) and aspect ratio (AR), which is defined as the ratio of R to average chord length ($\bar{c}$) for a single wing. In most cases, R is proportional to insect body length, but AR might range from 1 to 5 for different insect species [15]. Small AR typically implies less maneuverability but smaller wing loading, as displayed by butterflies. Consequently, most insects adopt moderate wing aspect ratios to find a balance between the wing loading and flight agility.

Obviously, it is not possible to fully describe the wing shape merely with R and AR as we can move the wing area longitudinally and transversely. Ellington [4] studied the relation between the radii of wing area for a variety of insects, birds and bats, and proposed to use the Beta probability density function (BPDF) to describe the spanwise area distribution. Two parameters of the BPDF, namely mean value and standard deviation, are equivalent to the non-dimensional first and second radius of moment of area, $\hat{r}_1$ and $\hat{r}_2$. His "laws of wing shape" show that there exists an approximate relationship between $\hat{r}_1$ and $\hat{r}_2$: $\hat{r}_2 = 0.929\hat{r}_1^{0.732}$. Hence, the spanwise area distribution can be characterized by a single parameter $\hat{r}_1$, which also indicates the spanwise centroid position and usually ranges from 0.4 to 0.6 for insect wings. Wang *et al.* [12] studied the effect of $\hat{r}_1$ on the optimal hovering kinematics and flight efficiency, and showed that locating more area towards the wing tip leads to more efficient hovering flight. However, their model ignored the power consumption resulting from the generated side force, which becomes more significant when more area is put close to the wing tip. Consequently, wings with moderate values for $\hat{r}_1$ are likely more energy efficient, for instance, the values of $\hat{r}_1$ for most Diptera insects are between 0.45 and 0.55 [4].

If we look at the insect wing shapes of different species, there are different percentages of wing area distributed in the front of the pitching axis. It is therefore necessary to introduce additional parameters to describe the chordwise area distribution. The non-dimensional length between the LE and pitching axis, $\hat{d}(r)$, which is normalized by the local strip length, is used to characterize the chordwise area distribution. For simplicity, the change of $\hat{d}$ along the span is assumed to be linear, which already enables to represent a huge number of wing shapes. Hence, we introduce shape parameters $\hat{d}_{\text{root}}$ and $\hat{d}_{\text{tip}}$ to define $\hat{d}(r)$.

With fully described wing shape, which is crucial for the passive pitching motion and power consumption, the moment of inertia ($\boldsymbol{I}$) can be determined if we know the mass distribution over the wing planform. For insect wings, the venation distribution dominates the mass distribution. The enrichment of veins at the wing root and near the pitching axis makes the mass distribution heterogeneous, which decreases the mo-

ment of inertia and, thus, the energy loss due to wing inertia. However, we still lack knowledge on the distribution of the wing mass for an arbitrary wing shape. Consequently, a uniformly distributed wing mass is hereby assumed.

2.2 *Flapping kinematic parameters*

The most significant characteristics separating the insect flight with fixed-wing and rotary-wing vehicle flight is that flying insects reciprocate their wings to exert moment on the surrounding air to produce lift and thrust. This reciprocating motion leads to a spanwise velocity gradient along the wing and continuously varying translational and rotational velocity during the periodic rotation of the wing. All these characteristics are crucial for the generation of sufficient aerodynamic forces for insects.

Considering the complexity of wing spatial movement, three Euler angles are generally used to describe the flapping kinematics. They are sweeping angle ϕ (yaw), heaving angle θ (roll) and pitching angle η (pitch), as illustrated in Figure 2. Two coordinate systems (CSs) are of particular interest for the study of flapping wing motion, i.e. the inertial CS $x_i y_i z_i$ and the co-rotating CS $x_c y_c z_c$, which are fixed on the body and wing, respectively. Both CSs are shown in Figure 2. Aerodynamic forces are preferably calculated in the co-rotating CS and subsequently transformed into the inertial CS to evaluate whether the wing design is able to produce sufficient lift and thrust or not. The power consumption is also calculated in the co-rotating CS since the wing moment of inertia does not change with wing flapping.

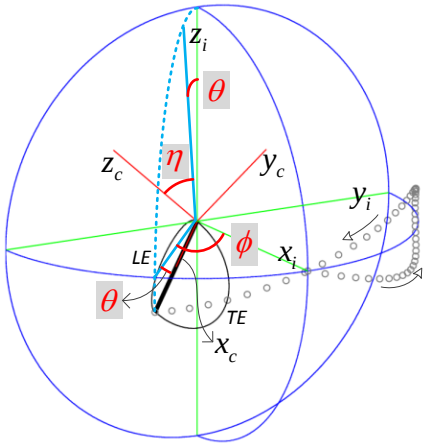

Figure 2: Definition of Euler angles for studying flapping-wing kinematics.

In nature, a variety of wing tip trajectories can be found, and a collection was done by Berman and Wang [10]. Most wing tip trajectories can be categorized as three types, i.e., "∞" shape, "$\smile$" or "$\frown$" shape and "$-$" shape. The shape of "$-$" implies that no heaving motion is existent, and it is the most frequently used kinematic pattern by FWMAVs. In order to quantitatively describe these tip trajectories, the mathematical representation with three Euler angles is necessary.

The wingbeat frequency (f) of different flying insects exhibits huge differences, ranging over three orders of magnitude from 5.5 Hz (Damselfly) to 1046 Hz (Chironomoidea) [15]. Generally, f varies inversely with wing inertial loads [16], especially for those insects exploiting resonant systems to flap their wings. That is coincident with our intuitive feeling about flying insects. For instance, larger insects usually flap their wings more slowly, and insects with small aspect ratio wings (e.g., butterfly) also fly with relatively low f as compared to those with comparative body mass and wing span. Additionally, if the flying circumstance does not vary a lot, the flapping frequencies of individual insect species are fairly constant, and their variation coefficients are within 5% for insects in hovering flight as studied by Ellington [17]. This can be partly explained by the exploitation of the resonant drive system by insects. Insects prefer to flap their wings at the resonant frequency to save energy.

Insects reciprocate their wings with quite different stroke amplitudes, which could range from 66° for the Syrphid fly [17] to 180° or even higher for some beetles and moths [15]. Several studies [10, 12] show that higher stroke amplitude is beneficial for a more efficient flight. However, some limitations constrain the stroke amplitude to achieve or exceed 180°. These constraints include the geometric constraint due to wing-body interference and physical constraint of the wing-driving apparatus of insects or FWMAVs. The sweeping motions of insect flight are usually in a sinusoidal or near sinusoidal pattern, while some flapping-wing drive mechanisms [18, 19] generate sweeping motions in a triangular pattern. The triangular sweeping motions experience quick reversals between half-strokes and fairly constant wing translational velocities. Taha *et al.* [20] found that a triangular waveform sweeping angle and a constant pitching angle throughout the half-stroke yield the optimal performance while only aerodynamic power is considered. However, that specific pitching motion is hard to generate. The kinematics of some insect flights also shows an asymmetric downstroke and upstroke, but symmetric sweeping motion is more general in hovering flights of insects and FWMAVs. In order to generate a pitching moment for flight control, some insects [7] and FWMAVs [21] adopt offset sweeping motions, where the centerline of the sweeping motion angles to the front or rear. Here, we use the model proposed by Berman and Wang [10] to describe the sweeping motion for hovering flight:

$$\phi(t) = \frac{\phi_m}{\arcsin K} \arcsin\left[K \sin(2\pi f t)\right] + \phi_0, \qquad (1)$$

where ϕ_m and ϕ_0 are the sweeping amplitude and horizontal offset, respectively, and K ($0 < K < 1$) is a parameter used to control the shape of the sweeping motion: if $K \to 0$, $\phi(t)$ becomes a sinusoidal pattern, and if $K \to 1$, $\phi(t)$ becomes triangular .

To describe the out-of-plane movement of flapping wings, the heaving angle θ is described by a sinusoidal function,

$$\theta(t) = \theta_m \sin\left(2\pi N f t + \Phi_0\right) + \theta_0, \tag{2}$$

where N takes either 1 for the "$\smile$" or "$\frown$" shape or 2 for the "∞" shape, and θ_m, Φ_0 and ϕ_0 are the sweeping amplitude, vertical phase shift and vertical offset, respectively.

Pitching angle (η) provides the information of the geometric angle of attack (AOA) (α_{geo}), e.g., $\alpha_{\text{geo}} = 90^\circ - |\eta|$ if there exists no heaving motion. Together with the induced velocity and translational forward velocity, the effective AOA (α_{eff}) can be obtained. The pitching angle demonstrated in insect's flight mainly originates from the wing deformation, which is a combination of wing bending, camber and torsion. This deformation is determined by distributed wing stiffness and wing inertia as well as aerodynamic loads. In this paper, the distributed wing stiffness is replaced by the rotational stiffness of the torsional spring based on the rigid wing model. Since the wing inertia can be calculated easily in the co-rotating CS, the calculation of transient aerodynamic loads is the key to simulate the passive pitching motion.

A quasi-steady aerodynamic model is used to calculate the transient aerodynamic loads. The loads are decomposed into four components that originate from different sources: wing translational velocity, rotational velocity, coupling between the wing translational and rotational velocities, and added mass effect, as illustrated in Figure 3. Specifically, we use an analytical model proposed by Taha *et al*. [22] to calculate the loads due to the wing translational velocity. The analytical model enables the calculation of the lift coefficient for a translational 3-D wing with arbitrary aspect ratio, which facilitates the aerodynamic analysis of different wing shapes. By contrast, previous quasi-steady models [23, 24] estimated the wing translational loads with empirical data from experimental measurements on specific insect-wing-like mechanical wings, which restricts its application to different wing shapes. Although the wing rotational velocity does not contribute to the average forces over a cycle with two symmetric half-strokes, it is an important part of the transient damping torque around the pitching axis and, thus, included in our model. If the pitching axis is located at the chord center, no net transient force results from the wing rotational velocity. However, there still exists an additional force, which is a result of the coupling effect between the wing translational and rotational velocities [23, 25]. An analytical formula proposed by Fung [26] for an oscillating plate with small AOA shows a good prediction of the force due to the coupling and, thus, is used in our model. The center of pressure due to the coupling is at the 3/4 chord length from LE. The quasi-steady model including the damping torque from this term shows a better agreement with measured the passive pitching motion in experiments than the model without this term [27]. The added mass effect is due to the wing acceleration or deceleration, which leads the surrounding air to be accelerated or decelerated as well. The disturbed air will, in turn, exert forces on the wing.

Because of the variation in the velocity and acceleration along the wing span, the blade-element method [28], which discretizes the wing into infinitesimal chordwise strips, is used together with the quasi-steady model. The loads in the co-rotating CS can be calculated by integrating the loads on each of the strips over the entire wing. The average loads can be obtained by averaging the transient forces over a stroke cycle.

According to Euler's second law of motion for a rigid body, the external torque about the axis x_c is equal to the time derivative of angular momentum about the same axis,

$$\tau_{x_c}^{\text{aero}} + \tau_{x_c}^{\text{spring}} = \frac{dL_{x_c}}{dt}, \tag{3}$$

where L_{x_c} is the x_c component of angular momentum $\boldsymbol{L}$ of the wing expressed in the co-rotating CS, which is equal to $\boldsymbol{I\omega}_c$, where $\boldsymbol{\omega}_c$ represents the angular velocity of the wing in the co-rotating CS. Then, the equation of motion for the passive wing pitching can be derived as:

$$\begin{aligned} I_{x_c x_c}\ddot{\eta} = &- k_\eta \eta + \tau_{x_c}^{\text{aero}} + I_{x_c x_c}\left[\tfrac{1}{2}\dot{\phi}^2 \cos^2\theta \sin(2\eta)\right. \\ &- \tfrac{1}{2}\dot{\theta}^2 \sin(2\eta) + 2\dot{\phi}\dot{\theta}\cos\theta\cos^2\eta + \ddot{\phi}\sin\theta\left.\right] \\ &+ I_{x_c z_c}\left[\ddot{\theta}\sin\eta + \tfrac{1}{2}\dot{\phi}^2\sin(2\theta)\sin\eta\right. \\ &- \ddot{\phi}\cos\theta\cos\eta + 2\dot{\phi}\dot{\theta}\sin\theta\cos\eta\left.\right], \end{aligned} \tag{4}$$

where $\tau_{x_c}^{\text{aero}}$ is an implicit function of η, $\dot{\eta}$ and $\ddot{\eta}$. Then, the pitching angle can be obtained by numerically solving this second order ordinary differential equation. Using the quasi-steady aerodynamic model and the resulting kinematics, an analysis of the effects of the parameters on the lift generation and power consumption can be conducted.

3 Analysis of Design Parameters

3.1 Preliminary analysis

The majority of parameters discussed above have been studied from the lift and thrust generation perspectives [5, 10, 12, 29, 30]. For instance, longer wing span, higher flapping frequency and larger sweeping amplitude tend to generate more lift force. A medium value of the pitching amplitude ($40^\circ - 60^\circ$) also benefits the lift generation. Heaving motion is likely to enhance lift generation, since the plunging after wing reversals can increase the effective AOA. However, the influence of these shape and kinematics parameters on the power efficiency is not clear. Therefore, it is necessary to explore how to select these parameters for a more efficient flight, which is important for designing FWMAVs.

Power consumed by flapping flight mainly consists of four parts: profile power (P_{pro}), parasitic power (P_{par}), induced power (P_{ind}) and inertial power (P_{iner}). The first three can be categorized as aerodynamic power (P_{aero}). Specifically, P_{pro} results from the work done to overcome the drag

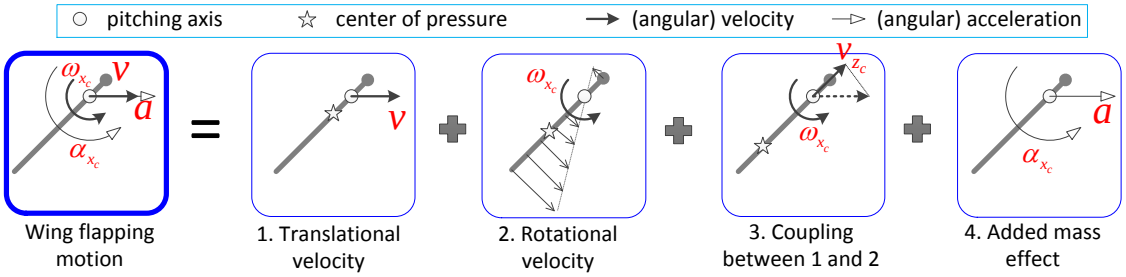

Figure 3: Decomposition of the quasi-steady aerodynamic modeling. The gray line and filled circled represent the wing chords and leading edge, respectively.

Parameters	Descriptions	Design domain in optimization	Ranges of parameters in sensitity analysis
$\hat{r}_1$	normalized radius of first moment of area	0.45	[0.4, 0.6]
R [m]	wing span	0.05	[0.045, 0.055]
AR*	aspect ratio	[1, 4]	[1,4]
$\hat{d}_{\text{root}}$*	$\hat{d}$ at the wing root	[0, 0.5]	[0, 0.5]
$\hat{d}_{\text{tip}}$*	$\hat{d}$ at the wing tip	[0, 0.5]	[0, 0.5]
k_η [Nm/rad]*	rotational stiffness	$10^{-4} \times [1, 15]$	$10^{-4} \times [1, 15]$
f [Hz]*	flapping frequency	[5, 30]	[5, 30]
ϕ_m[rad]	sweeping amplitude	$\{\pi/4, \pi/3, \pi/2\}$	$\{\pi/4, \pi/3, \pi/2\}$
K	control sweeping pattern	0.01	[0.01, 0.99]
ϕ_0 [rad]	horizontal offset	0	$[-\pi/30, \pi/30]$
θ_m [rad]	heaving amplitude	0	$[0, \pi/6]$
Φ_θ [rad]	heaving phase shift	0	$[-\pi, \pi]$
θ_0 [rad]	vertical offset	0	$[-\pi/10, \pi/10]$
N	control wing tip trajectory	0	2

Table 1: List of parameters, their domains in optimization and sensitivity analysis. Parameters labeled with "*" are selected as design variables in optimization. The design domains in optimization refer to the frequently studied insects (moths, beetles) and FWMAVs.

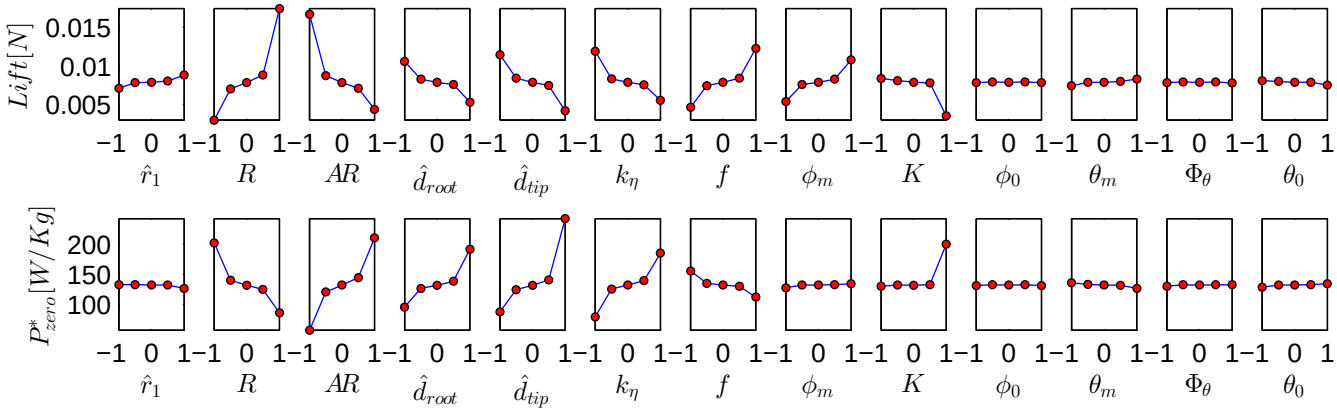

Figure 4: Importance comparison of design parameters in response to lift and power consumption P^*_{zero}. The values "-1" and "1" represent the selected lower and higher setting of each design parameters. These filled circles in red indicate the mean lift or power consumption of all the trials while fixing the corresponding parameter at certain level.

on the wing. P_{par} is the power required to overcome drag on the body, which is negligible for hovering flight but significant for high-speed forward flight. P_{ind} is expended to overcome the drag on the wing due to induced downwash velocity which was estimated by the (partial) actuator-disk model [31]. However, this model does not consider any unsteady aerodynamic effects, which makes it not accurate to estimate the P_{ind}. Nevertheless, P_{ind} is generally less than 20% of the total power [32] and does not vary a lot with the wing morphology and kinematics, except for the stroke amplitude. Thus, P_{ind} is ignored in the analysis of the effect of these design parameters on power efficiency. Additional to aerodynamic power expenditure, P_{iner} is required to accelerate the wing mass and virtual mass due to accelerated surrounding air in the first half of a half-stroke. In the second half, the decelerating wing will lose its kinetic energy, which might be used to overcome aerodynamic drag or stored in the cuticle, flight muscles and resilin for insects [15] or elastic structure of FWMAVs [2]. This kinetic energy might also be dissipated by the thorax structure, which makes the power efficiency of flapping flight hard to determine. In this paper, two patterns of power consumption are studied:

- Perfect energy storage, which means all kinetic energy can be either used to compensate the power consumed by the drag or recycled by the drive mechanism, termed as P_{per}.
- Zero energy storage but perfect energy transfer between inertial and aerodynamic work, which implies that if stored kinetic energy in the first half of a half-stroke is less than P_{aero} required for the second half of the half-stroke, all the inertial power is fully recycled and total power is equal to P_{per}, otherwise, part of the kinetic energy will be dissipated. It is denoted as P_{zero}.

The power consumption of flapping flight generally lies between P_{per} and P_{zero}. To facilitate the comparison of energy-efficiency between different flapping-wings, the power consumption is normalized by the transient lift (in kilograms, if negative taking the absolute value) and denoted with an asterisk, e.g., normalized aerodynamic power consumption $P^{\star}_{\text{aero}}$.

In Table 1, all the design parameters are listed. To gain insight into the importance of these parameters to the lift generation and power consumption, the screening of these parameters with 5-level fractional factorial experimental design approach [33] is first carried out. It can be seen from Figure 4 that: R, AR, $\hat{d}_{\text{root}}$, $\hat{d}_{\text{tip}}$, f and k_η have more influence on both lift generation and power consumption than $\hat{r}_1$, ϕ_0 and all the heaving motion parameters. ϕ_m shows relatively more influence on lift generation than on power consumption. Although the interaction and higher-order terms of these parameters are not included in the screening, the results provide a rough picture of parameters that should be included in the design variables in optimization.

Table 2: Optimization results.

ϕ_m	$\pi/4$	$\pi/4$	$\pi/3$	$\pi/3$	$\pi/2$	$\pi/2$
P^*_{per}	16.46	–	18.89	–	23.40	–
P^*_{zero}	–	21.53	–	23.93	–	27.70
AR	1.00	1.00	1.00	1.00	1.00	1.00
$\hat{d}_{\text{root}}$	0.12	0.26	0.12	0.14	0.18	0.24
$\hat{d}_{\text{tip}}$	0.42	0.22	0.48	0.22	0.39	0.08
k_η	1.32	1.15	1.03	1.25	0.82	1.01
$(\times 10^{-3})$						
f	14.74	13.89	13.19	11.88	10.41	9.80
$\eta_m(^\circ)$	43.63	49.67	46.69	50.25	52.36	55.62

3.2 Optimization

The optimization is set up to search for the combination of wing shape and flapping kinematics with the least power consumption but with the minimal lift generation (1[g]) for a single wing. To make the optimization meaningful and manageable, some parameters are prescribed similar to the size of an adult Hawk moth, which are frequently used by FWMAVs [2, 34]. R and $\hat{r}_1$ are set as 50 [mm] and 0.45, respectively; the average wing density is set to 0.05 $[Kg/m^2]$; three discrete values $\pi/4$, $\pi/3$ and $\pi/2$ are considered for ϕ_m of a harmonic sweeping motion with $K = 0.01$; ϕ_0 and the heaving motion are ignored in optimization. For the other five design parameters, i.e., AR, $\hat{d}_{\text{root}}$, $\hat{d}_{\text{tip}}$, k_η and f, optimization is carried out to search for the most energy-efficient combination of these parameters corresponding to both power patterns.

Given that solving the ODE (Eq. 4) may have convergence problem and the power defined in the design domain is a non-convex set, a global optimization method is used to search for a rough solution. Next, a response surface is fitted around the rough optimum with using a cubic spline, based on which the gradient-based optimization is carried out for the determination of the optimum.

For a rigid wing with uniform mass distribution, the optimal combinations of wing shape and kinematics for hovering flight without heaving motion are listed in Table 2 with respect to three discrete sweeping amplitudes. From the results it can be concluded that:

1 Relative to adult Hawk moths, wings with minimal aspect ratios ($AR = 1$) are obtained, as shown in Figure 5. A smaller AR increases the wing area and, thus, the lift generation. However, the power consumption also increases due to the increase of wing inertia. Both the optimal location of the pitching axis and flapping frequency are used to compensate the increased power consumption due to the smaller AR. The optimal pitching axis is located close to the wing center line and center of pressure, which is located between 1/4 and 1/2 chord length from LE. Meanwhile, smaller flapping frequencies, especially for P^*_{zero}, are also found by optimization. These optimal wing shapes suggest

that having wing area in front of the pitching axis is more energy-efficient than those with straight leading edges as the pitching axis. The latter designs are quite commonly used for artificial wings of FWMAVs.

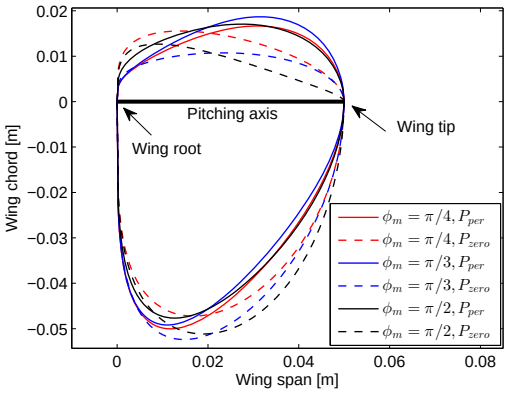

Figure 5: Optimal wing shape for both power patterns with three different sweeping amplitudes.

2 The optimal flapping frequencies are inversely proportional to the sweeping amplitudes. The power consumption with respect to the optimal design increases with the sweeping amplitude when the induced power is ignored. This conclusion is different from that obtained for the flapping motion with fully active kinematics [10, 12], which shows that a larger sweeping amplitude is more energy efficient. To achieve the optimal pitching amplitudes (η_m), as listed in the last row of Table 2, the spring stiffness (k_η) is tuned to different values.

3.3 Sensitivity analysis

Sensitivities of the lift and power consumption for single parameters for both power patterns, with $\phi_m = \pi/3$, are plotted in Figure 6 and 7. The sensitivities plotted in subplots from (a) to (i) are calculated based on the prescribed values of $\hat{r}_1$, R, K and ϕ_0, and the optimal values of five design variables in the optimization without considering the heaving motion.

For both power patterns, an increase of $\hat{r}_1$ or R does not always generate higher lift and reduce energy efficiency if the pitching axis and rotational stiffness are fixed, since there exists an optimal moment of inertia that is related to $\hat{r}_1$ or R which gives rise to the preferable passive pitching amplitude. According to sensitivities in subplots from (c) to (g) for both power patterns, the optimal design obtained with the objective of the minimal power consumption are approximately coincident with the optimal design for the maximal lift generation. With the increase of parameter K, as shown in subplot (h), both the lift and mass-normalized power decrease for the power pattern P^*_{per}, but for P^*_{zero} the power decreases between 0.01 and 0.9 and then increases due to high wing inertia at the fast wing reversal phase. From subplot (i) in both figures, it can be found that the horizontal offset of the stroke plane has no influence on the aerodynamic force generation or power consumption. However, the location where the average lift is located with respect to the center of mass will move and, thus, the moment around the center of mass will change. This is useful for flight control.

To study the effect of heaving motion parameters on the lift and power consumption, first, the heaving amplitude θ_m is varied between 0 and $\pi/6$. Then, by setting θ_m as $\pi/10$, the sensitivities with respect to Φ_θ and θ_0 are calculated and plotted in subplots (k) and (l). It can be seen that hovering performance can be improve by turning these three parameters, although a more complicated drive system is required to achieve the desired heaving motion.

The peaks of power consumption in subplots (f) and (g), which are no shown, are due to the absolute value of transient lift, which is used to normalize the power, getting close to zero. For other cases with different sweeping amplitudes, the results of sensitivities are not shown as no significant difference with Figures 6 and 7 is found.

4 Conclusions

Passive pitching motion is preferable for flapping wing design since it simplifies the drive mechanism, saves energy and reduces structural weight. The passive pitching is related to both the wing shape and flapping kinematics, which requires the combined design of these two aspects. To obtain an insight into the effect of these parameters on lift and power consumption, five shape parameters and seven kinematics parameters as well the stiffness of the torsional spring have been studied. The passive pitching motion is simulated based on a rigid wing model and a quasi-steady aerodynamic model. Based on the importance analysis of these parameters, five parameters, including AR, $\hat{d}_{\text{root}}$, $\hat{d}_{\text{tip}}$, k_η and f, are selected as design variables in optimization while other parameters are prescribed.

Optimization results show that smaller aspect ratio wings with the pitching axis located close to the center of pressure and wing center line are more energy-effficient regardless of the elastic energy storage. Smaller power consumption can be achieved by the optimal wing design with smaller sweeping amplitude. Sensitivity analysis to all the design parameters shows the effect of these parameters on the lift and power consumption, which can assist in the selection of wing shape and kinematics pattern and help determine effective control parameters using the lift sensitivities.

This work is based on the assumption of a rigid wing model with uniformly distributed mass over the wing surface, which facilitates the comparison of different wing designs. Although this simplified model can not completely characterize the complexed morphology of insect wings, the optimal wing shapes and kinematics show the dependence of the performance on the moment of inertia of the wings and can be

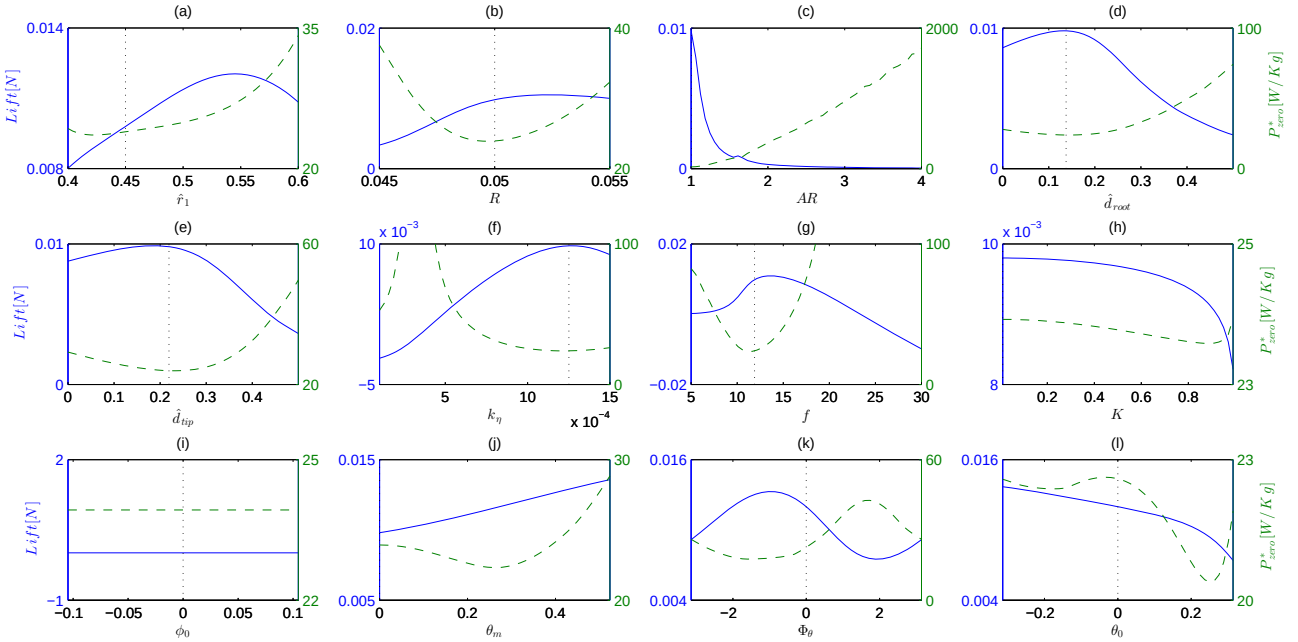

Figure 6: Effect of single parameters on the lift (solid line) and the power pattern P^*_{zero} (dashed line) while $\phi_m = \pi/3$. The values on x axes corresponding to dotted lines are either the optima from optimization (subplots (c)-(g)) or the prescribed values in optimization in other subplots. The dotted lines in subplots (k) and (j) overlap with left vertical axes. The sensitivities with respect to Φ_θ and θ_0 are calculated while set θ_m as $\pi/10$.

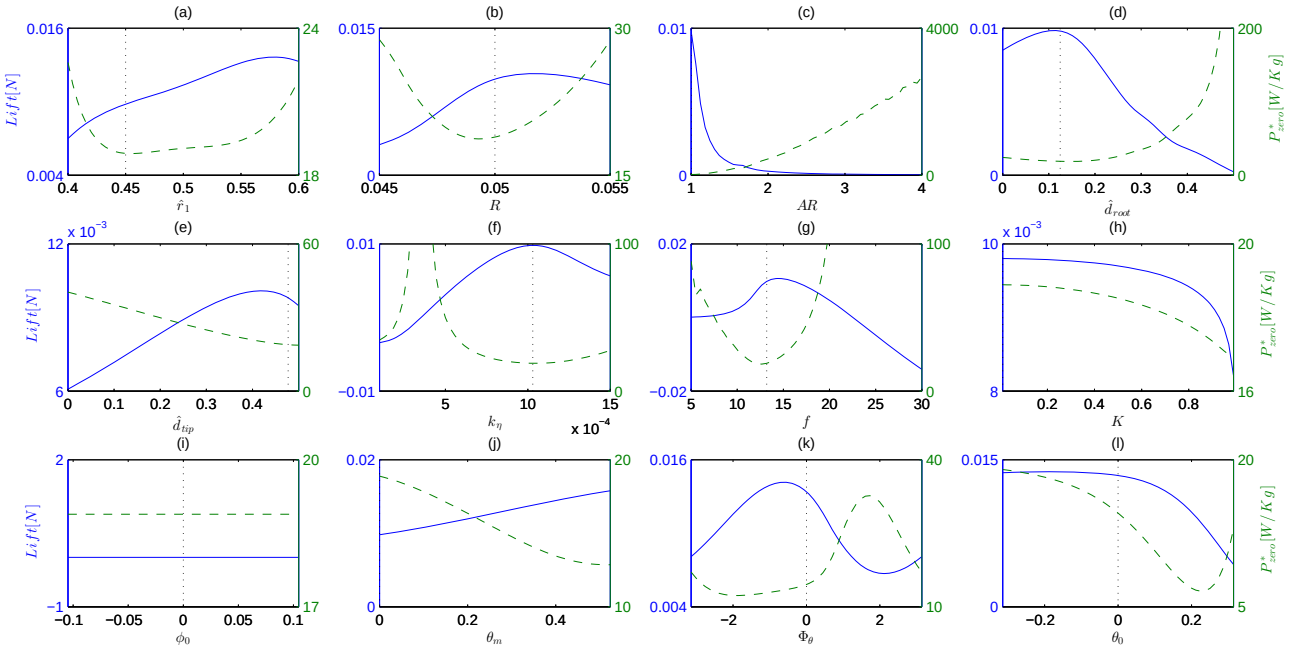

Figure 7: Effect of single parameters on the power pattern P^*_{per} while $\phi_m = \pi/3$. Details as in Figure 6.

used in the FWMAV design. In future, it is helpful to include forward flight and maneuvering as well to achieve more comprehensive understanding of these design parameters on the flight performance. In addition, wing torsion resulting from distributed wing stiffness is likely to further reduce the power consumption and should be considered in future modeling as well.

ACKNOWLEDGEMENTS

We would like to thank the China Scholarship Council for their financial support.

REFERENCES

[1] G. C. H. E. de Croon, K. M. E. de Clercq, R. Ruijsink, B. Remes, and C. de Wagter. Design, aerodynamics, and vision-based control of the DelFly. *International Journal of Micro Air Vehicles*, 1(2):71–98, 2009.

[2] C. T. Bolsman, J. F. L. Goosen, and F. van Keulen. Design Overview of a Resonant Wing Actuation Mechanism for Application in Flapping Wing MAVs. *International Journal of Micro Air Vehicles*, 1(4):263–272, December 2009.

[3] K. Y. Ma, P. Chirarattananon, S. B. Fuller, and R. J. Wood. Controlled Flight of a Biologically Inspired, Insect-Scale Robot. *Science*, 340(6132):603–607, May 2013.

[4] C. P. Ellington. The Aerodynamics of Hovering Insect Flight. II. Morphological Parameters. *Philosophical Transactions of the Royal Society B: Biological Sciences*, 305(1122):17–40, February 1984.

[5] R. J. Wootton. Functional morphology of insect wings. *Annu. Rev. Entomol.*, 37:113–140, 1992.

[6] R. Dudley and C. P. Ellington. Mechanics of Forward Flight in Bumblebees: I. Kinematics and Morphology. *J. Exp. Biol.*, 148(1):19–52, January 1990.

[7] A. P. Willmott and C. P. Ellington. The mechanics of flight in the hawkmoth Manduca sexta. I. Kinematics of hovering and forward flight. *J. Exp. Biol.*, 200(21):2705–2722, November 1997.

[8] A. P. Willmott and C. P. Ellington. The mechanics of flight in the hawkmoth Manduca sexta. II. Aerodynamic consequences of kinematic and morphological variation. *Journal of Experimental Biology*, 200(21):2723–2745, November 1997.

[9] T. L. Hedrick and T. L. Daniel. Flight control in the hawkmoth Manduca sexta: the inverse problem of hovering. *The Journal of experimental biology*, 209(Pt 16):3114–30, August 2006.

[10] G. J. Berman and Z. J. Wang. Energy-minimizing kinematics in hovering insect flight. *Journal of Fluid Mechanics*, 582:153, June 2007.

[11] J. P. Whitney. *Design and Performance of Insect-Scale Flapping-Wing Vehicles*. Phd thesis, Harvard University, 2012.

[12] Q. Wang, J. F. L. Goosen, and F. van Keulen. Optimal hovering kinematics with respect to various flapping-wing shapes. In *IMAV 2013*, Toulouse, France, 2013.

[13] R. Å ke Norberg. The pterostigma of insect wings an inertial regulator of wing pitch. *Journal of Comparative Physiology*, 81(1):9–22, 1972.

[14] A. J. Bergou, S. Xu, and Z. J. Wang. Passive wing pitch reversal in insect flight. *Journal of Fluid Mechanics*, 591:321–337, October 2007.

[15] R. Dudley. *The biomechanics of insect flight: form, function, evolution*. Princeton University Press, 2002.

[16] O. Sotavalta. Flight-tone and wing-stroke frequency of insects and the dynamics of insect flight. *Nature*, pages 1057–1058, 1952.

[17] C. P. Ellington. The Aerodynamics of Hovering Insect Flight. III. Kinematics. *Philosophical Transactions of the Royal Society B: Biological Sciences*, 305(1122):145–181, February 1984.

[18] S. P. Sane and M. H. Dickinson. The control of flight force by a flapping wing: lift and drag production. *J. Exp. Biol.*, 204(15):2607–2626, August 2001.

[19] J. F. L. Goosen, H. J. Peters, Q. Wang, P. Tiso, and F. van Keulen. Resonance Based Flapping Wing Micro Air Vehicle. In *International Micro Air Vehicle Conference and Flight Competition (IMAV2013)*, number September, pages 1–8, Toulouse, France, 2013.

[20] H. E. Taha, M. R. Hajj, and A. H. Nayfeh. Wing Kinematics Optimization for Hovering Micro Air Vehicles Using Calculus of Variation. *Journal of Aircraft*, 50(2):610–614, March 2013.

[21] T. Q. Truong, V. H. Phan, S. P. Sane, and H. C. Park. Pitching Moment Generation in an Insect-Mimicking Flapping-Wing System. *Journal of Bionic Engineering*, 11(1):36–51, January 2014.

[22] H. E. Taha, M. R. Hajj, and P. S. Beran. State-space representation of the unsteady aerodynamics of flapping flight. *Aerospace Science and Technology*, 34:1–11, April 2014.

[23] S. P. Sane and M. H. Dickinson. The aerodynamic effects of wing rotation and a revised quasi-steady model of flapping flight. *J. Exp. Biol.*, 205(8):1087–1096, April 2002.

[24] A. Andersen, U. Pesavento, and Z. J. Wang. Unsteady aerodynamics of fluttering and tumbling plates. *Journal of Fluid Mechanics*, 541:65–90, October 2005.

[25] M. H. Dickinson, F. O. Lehmann, and S. P. Sane. Wing rotation and the aerodynamic basis of insect flight. *Science*, 284(5422):1954–1960, June 1999.

[26] Y. C. Fung. *An Introduction to the Theory of Aeroelasticity*. Courier Dover Publications, 1993.

[27] J. P. Whitney and R. J. Wood. Aeromechanics of passive rotation in flapping flight. *Journal of Fluid Mechanics*, 660:197–220, July 2010.

[28] M. F. M. Osborne. Aerodynamics of flapping flight with application to insects. *Journal of Experimental Biology*, 28:221–245, 1951.

[29] H. Liu. Integrated modeling of insect flight: From morphology, kinematics to aerodynamics. *Journal of Computational Physics*, 228(2):439–459, February 2009.

[30] H. J. Peters, J. F. L. Goosen, and F. van Keulen. Flapping wing performance related to wing planform and wing kinematics. In *12th AIAA Aviation Technology, Integration, and Operations (ATIO) Conference and 14th AIAA/ISSM*, volume 31, pages 1–11, Indianapolis, Indiana, 2012.

[31] T Weis-Fogh. Energetics of hovering flight in hummingbirds and in Drosophila. *Journal of Experimental Biology*, pages 79–104, 1972.

[32] M. Sun. High-lift generation and power requirements of insect flight. *Fluid Dynamics Research*, 37(1-2):21–39, July 2005.

[33] NIST/SEMATECH. e-Handbook of Statistical Methods, http://www.itl.nist.gov/div898/handbook/.

[34] DelFly Micro. http://www.delfly.nl/micro.html.